HNPS Advances in Nuclear Physics

Vol 10 (1999)

HNPS1999

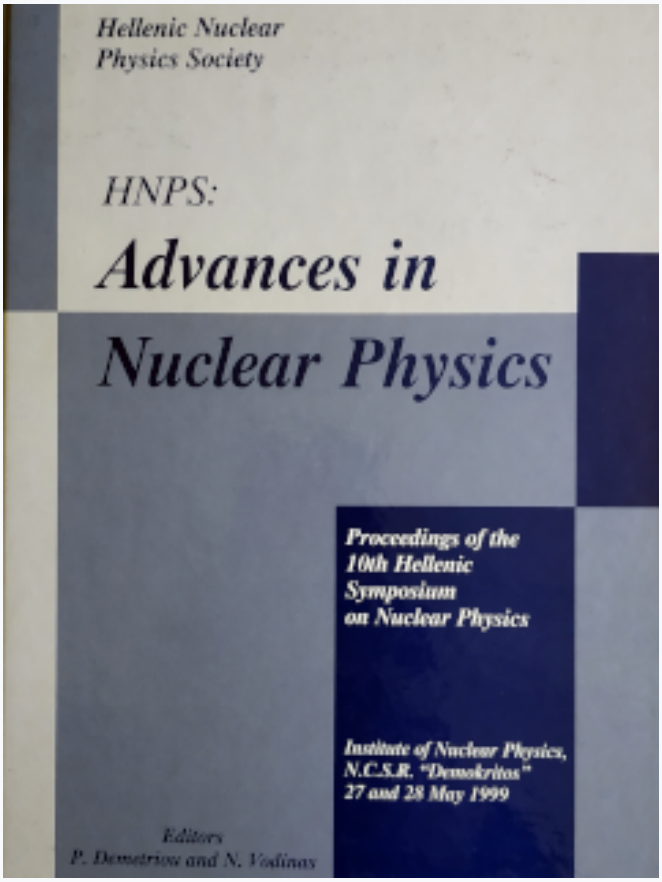


**Determination of Sulfur and Copper Profile with nuclear reactions**

*S. Kossionides, G. Kaliambakos, R. Vlastou, C. T. Papadopoulos*

doi: 10.12681/hnps.2168

# Determination of Sulfur and Copper Profile with nuclear reactions

S. Kossionides[a], G. Kaliambakos[a], R. Vlastou[b] and C.T. Papadopoulos[b]

[a] *Institute of Nuclear Physics, N.C.S.R. "Demokritos", GR-153 10 Aghia Paraskevi, Athens, Greece*

[b] *Department of Physics, National Technical University of Athens, GR-157 80 Zografou, Athens, Greece*

**Abstract**

The concentration and depth profile of Cu and S in patinna samples have been deternined by using Nuclear Reaction Analysis (NRA) and Rutherford Backscattering Spectroscopy (RBS). For the NRA the differential cross section was mesaured for the 1327 keV $\gamma$-ray deexciting the third excited state to the ground state of $^{63}$Cu through the reaction $^{63}$Cu(p,p'$\gamma$), as well as, for the 2230 keV $\gamma$-ray deexciting the first excited state to the ground state through the resonant reaction $^{32}$S(p,p'$\gamma$). The mesaurements of both excitation functions were performed in the energy range 3.0 - 3.7 MeV in 20 keV steps and at an angle of 125°.

## 1 Introduction

Copper and bronze artifacts, exhibited in public places (e.g. statues), form an essential part of the European cultural heritage. The composition of patinna on these artifacts is crucial for their preservation. Patinna consists of a combination of copper sulfate salts (such as brochandite $CuSO_43[Cu(OH)_2]$, antlerite $CuSO_42[Cu(OH)_2]$, etc.). In the frame of a European Collaboration artificial patinna samples were prepared and examined with various methods. The reactions $^{63}$Cu(p,p'$\gamma$) and $^{32}$S(p,p'$\gamma$) were used to obtain information on the distribution of the two elements and hence on the composition of the patinna layer. These nuclear reactions have also been used in the literature [1], [2] but either the targets were gaseous or the energy range was different. During the course of this work, it was attempted to use the data of [3] for the absolute value of the sulfur cross section, as well as the data of [4] for the angular distributions on the reaction resonances. It was found that the data from [3]

were taken with the Ge-Li detector placed at 90°, while our experimental data were taken at 125°, so we decided to remeasure the cross section of sulfur at that angle. In the same experiment we also measured the cross section of copper to confirm the data of the literature [5]. We report here on the measurements of the relevant cross sections and present several examples of their use for patinna analysis. Additional informations were obtained by using the RBS method for the depth profile of the heavier elements of the samples.

## 2 Experimental measurements

The patinna samples were obtained by courtesy of Prof. P. Missailides from Thessaloniki University. The experimental measurements that have been made concern irradiation of patinna samples with protons of energy 1.5 MeV for RBS measurements with a Si surface barrier detector placed at 160° with respect to the axis beam. Also protons of 3.375 - 3.700 MeV were used for (p,p'$\gamma$) measurements with the Ge-Li detector placed at 125°. With the same detector geometry, the cross sections for the (p,p'$\gamma$) reaction on Cu and S were also measured. To this purpose samples of pure copper and CdS respectively were irradiated with protons of energy 3.0 - 3.7 MeV with an energy step of 20 keV. The proton beam used for the irradiation was supplied by the Tandem T11/25 accelerator of the NRCPS "Demokritos" (figure 1), while data aquisition and control hardware were driven by a personal computer with the use of the appropriate software.

The incoming protons pass a $10\mu g/cm^2$C-foil, on which a thin gold layer of thickness 8,7±0,4 $\mu$gr/cm$^2$ was evaporated. The thickness of the Au-layer was determined with an XRF measurement. The foil was placed on the beam-target line and after passing through it, the protons fall on the target without substantial loss of energy or angular spread. The protons scattered off the foil, were detected by a Si detector, placed at an angle of 37° with respect to the beam. From the measured yield we calculated the total charge that falls on the target by using the cross section for Rutherford scattering of protons on Au. The relation we used for the calculation of charge is

$$A = \sigma \, \Omega \, I \, N \, \tau \tag{1}$$

where $A$ is the yield in number of counts; $\sigma$ is the Rutherford cross section for Au, which is given by $(Z_1 Z_2 e^2/4E) sin(\theta/2)^{-4} cm^2$ ($\theta$ is the angle of scattering in the lab system); $\Omega$ is the solid angle of the detector, which was 0.9 msr for the geometrical setup of our experiment; $I$ is the total number of incident particles on the target, which is more convenient to be expressed by the product $Q \times N_0$, where $Q$ is the charge in $\mu Cb$ and $N_0$ is equal to 6,25 $\times$ $10^{12}$ particles/$\mu$Cb in

the case of protons; $N$ is the atomic density of target Au, which is equal to 5,9 $\times 10^{22}$ at/cm$^3$ and finally $\tau$ is the thickness of Au foil in $\mu gr/cm^2$.

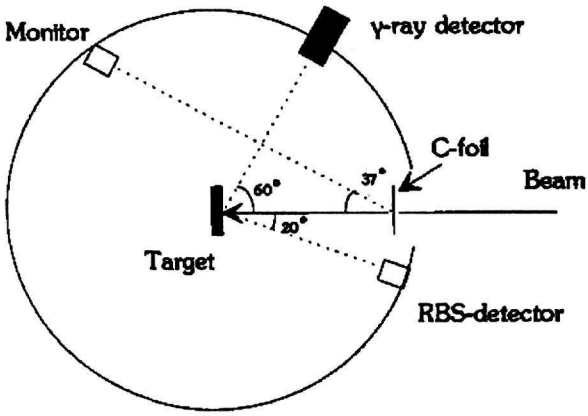


Fig. 1. Experimental setup for profile analysis.

## 3 Cross section calculation

In order to calculate the cross section for copper and sulfur, we used Eq (1) in reverse. From the yield of the reaction $A$ at an energy $E_0$ and the corresponding yield $A+\Delta A$ at an energy $E_0+\Delta E$ with the condition $\Delta E \ll E_0$ and providing the cross section changes very slowly with energy in that region, we find after integration and by using the relation $\Delta x = \Delta E/S(E)$, where $S(E)$ is the energy loss in units of $keV \cdot cm^2/\mu g$ for a target of reduced thickness $\Delta x$ in units of $\mu g/cm^2$, that

$$\sigma(E) = K \frac{\Delta A}{\Delta E} S(E) \tag{2}$$

where $K$ is a constant. In the case of $\gamma$-rays the measured counts are connected with the yield by the relation

$$Y = A \epsilon f w \tag{3}$$

where $\epsilon$ is the detector sensitivity, including the absolute efficiency of the detector and the geometrical solid angle. This parameter depends on the energy of the $\gamma$-rays. In the case where we have more than one isotopes of the element in the target, we must multiply with the isotopic abundance $f$ of the reacting

isotope, while in the existance of inactive atoms in the target, we multiply with the weight composition $w$ of the active element in the target.

From equations (1),(2) and (3) we finally have for the cross section

$$\sigma = \frac{\Delta Y}{\Delta E} \cdot \frac{B \cdot S(E)}{N_{Av}\, f\, w\, N_0\, Q\, \epsilon} \tag{4}$$

where B is the molecular weight of the target in gr/mole and $N_{Av}$ is the Avogadro number which equals to 6,023 $\times 10^{23}$ at/mole.

This relation gives the cross section for Cu for the case of non-resonant scattering we mentioned before. However, in the case of S, where we have isolated narrow resonances (all with width $\Gamma \ll \Delta E$), the previous relation is valid only for the non-resonant part of the reaction. For the resonant part, the cross section has the form of Breit-Wigner distribution [6]

$$\sigma(E) = \pi\lambda^2\omega \frac{\Gamma_i\Gamma_e}{(E - E_R)^2 + (\Gamma/2)^2} \tag{5}$$

where $\lambda$ is the De-Broglie wavelength, $\omega$ the statistical factor, $E_R$ the resonant energy and $\Gamma_i$, $\Gamma_e$ the partial widths for the inelastic and the elastic channel. When the energy width of the target is much greater than the total width of the resonance ($\Delta \gg \Gamma$), that is for the case of a thick target, the quantities $\lambda$, $\Gamma_i$, $\Gamma_e$, $S(E)$, $\Delta$ are practically constant in the resonance area and are determined by the value they have at $E = E_R$. So, for thick target measurements, the yield reaches a maximum value $Y_{max}(\infty)$ for $E_0 \gg E_R$, which represents the integral of the resonance over the entire region

$$Y_{max}(\infty) = \frac{\lambda_R^2}{2}\omega\gamma \frac{(M+m)}{M} \frac{1}{S(E)} \tag{6}$$

where $M$ is the mass of the target, $m$ the mass of the projectile and $\gamma = \Gamma_i\Gamma_e/\Gamma$.

In the case where the measurements are taken by a detector placed at an angle $\theta$ and subtending a solid angle $\Delta\Omega$, then only a percentage of the total yield of $\gamma$-rays is detected, which is given by the relation

$$N(\theta) = Y_{max}(\infty)\frac{N_{Av}}{B}\epsilon f W(\theta) \tag{7}$$

where $W(\theta)$ is the angular distribution of the $\gamma$-rays. If there also exist inactive atoms in the target, the energy loss $S(E)$ in Eq (6) must be multiplied by the

weigth percentage $w$ of the active element. Finally we have

$$N(\theta) = \frac{\lambda_R^2}{2}\omega\gamma\frac{(M+m)}{M}\frac{1}{wS(E)}Q\,N^*\,\epsilon\,W(\theta)\,\frac{N_{Av}}{B} \tag{8}$$

Furthermore, by integrating Eq (8) over the entire solid angle, the factor $W(\theta)$ is reduced to 4 $\pi A_0$ where $A_0$ is the coefficient of the zero order Legendre polynomial that enters the angular distribution, so the yield at the specific angle of detection 125° is given by the relation

$$Y(125°) = N(\theta)\frac{2\pi W(125°)}{4\pi A_0} \tag{9}$$

## 4 Copper Cross Section

In the case of copper, from Eq (4) we find the cross section for the non-elastic scattering $^{63}$Cu(p,p'$\gamma$) for the excitation energy at 1327 keV [7]. The choice of this excitation energy was made so that we have a correspondance with the depth where sulfur resonances are excited. Because of the small number of measured counts, the cross sections calculated with the method we mentioned above have large errors, so when we calculate the yield with the programme PGAMMA (code FORTRAN77) [8], we find deviations from the experimental values. In order to smooth out the cross section, we use a mean value approach whereby to a value of the cross section at a specific energy $E$ we add the cross sections at $E \pm \Delta E$ and take the mean value (for example as the cross section at 3200 keV we take the mean value of the cross sections at 3180, 3200 and 3220 keV). This is not an unreasonable approach, since the cross section for copper does not show any resonant behaviour at the energy region we study, but has a very small, smooth increase with energy. Thus the smoothening procedure gives rise to negligible errors [5]. Furthermore, to the resulting calculated yield we add the value of the yield at the lowest energy that we get experimentally (3 MeV), in order to take into account the contribution of the previous values of the cross section of Cu into the excitation function. As a result of the previous procedure we obtain an overall satisfactory agreement between the cross section found by [5] and the cross section that is reproduced by our measurements. So we can use this modified cross section (Fig. 2) in our analysis.

## 5 Sulfur Cross Section

Eq (9) gives the calculated yield of the reaction $^{32}$S(p,p'$\gamma$) in the energy region $E \gg E_R$ for $CdS$, with $MB$ equal to 144,46 g/mole and $w$ equal to 0,222 for

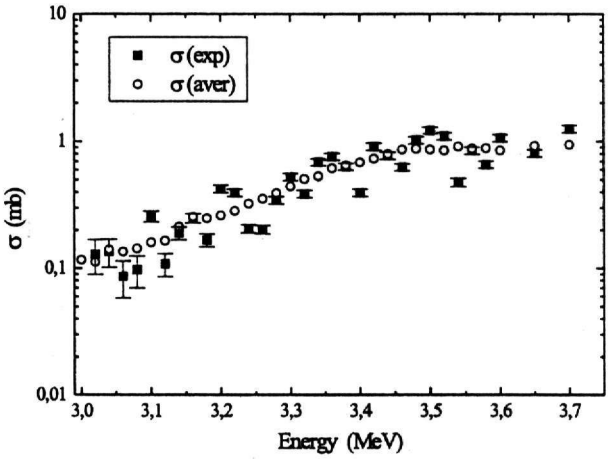


Fig. 2. Average experimental and calculated cross section of the reaction $^{63}Cu(p,p'\gamma)$.

CdS; $(M+m)/M$ is equal to 1,032 and $\epsilon$(2230 keV) was found $4{,}26\times10^{-4}$. Taking into account the values of W($\theta$) and $A_0$ in the literature [4],we obtain the values shown in Table 1.

Table 1
Values of the resonant parameters $\lambda_R^2, S(E), W(120°)$ and $A_0$.

| E(keV) | $\lambda_R^2(cm^2)$ | $S(E)$ $(keV\cdot cm^2/\mu g)$ | $W(120°)$ | $A_0$ |
|---|---|---|---|---|
| 3094 | $2{,}73\times10^{-24}$ | 0,05554 | 0,826 | 0,9578 |
| 3195 | $2{,}65\times10^{-24}$ | 0,05463 | 2,278 | 2,0272 |
| 3379 | $2{,}50\times10^{-24}$ | 0,05300 | 1,687 | 1,5963 |

From the literature [3,4] and the relations $\gamma = \Gamma_i\Gamma_e/\Gamma$ and $\omega = (2J_1+1)/(2s+1)(2J_0+1)$ , we find the values for the $\omega\gamma$ of each resonance shown in Table 2. We also represent the resulting yields for the three resonances with their error, together with the experimentally measured yields, which as we can see agree with the calculated values within the error range. The yield units are counts/$\mu$ Cb.

From Eq (4) we obtain the values for the cross section. If we assume that apart from the cross section values at 3120, 3220 and 3400 keV (where we observe the highest contribution from the 3 resonances) the rest of the cross section values are non-resonant without significant error, then by inserting them as input to the programme PGAMMA we calculate the yield that comes exclusively from the non-resonant part of the reaction $^{32}$S(p,p'$\gamma$). If we add

Table 2
Width Γ, strength $\omega\gamma$ and yield Y of the three resonances.

| $E_R$ (keV) | Γ (keV) | $\omega\gamma$ (keV) | $Y_{th}$ | $Y_{exp}$ |
|---|---|---|---|---|
| 3094 | 0,34 ± 0,20 | 0,0605 ± 0,0107 | 32 ± 7 | 26,0 ± 3,8 |
| 3195 | 0,44 ± 0,08 | 0,0098 ± 0,0018 | 7± 1 | 6,0 ± 0,3 |
| 3379 | 1,00 ± 0,20 | 0,320 ± 0,064 | 206± 40 | 191 ± 7 |

to this non-resonant yield the values of the resonant yields that correspond to the three resonances, we obtain the excitation yield of the resonant reaction $^{32}$S(p,p'$\gamma$). By comparing this with the experimentally measured, we see very good agreement (figure 5). Also in Table 3 we have the non-resonant cross section for the energy range 3 - 3,7 MeV.

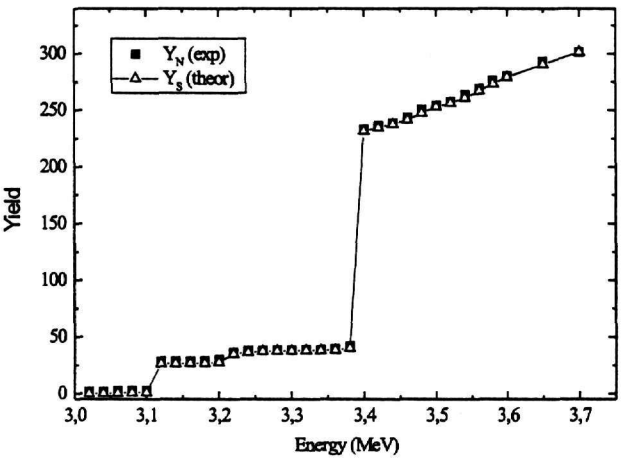


Fig. 3. Excitation function for the reaction $^{32}$S(p,p'$\gamma$).

## 6 Application on patinna samples

Using the cross sections for sulfur and copper which we measured we can now calculate, using the programm PGAMMA the composition of Cu and S with depth for various samples for which we have measured the yield in counts at the peaks at 1327 (for copper) and 2230 keV (for sulfur) respectively. Modifying the composition of S and (or) Cu and the thickness of the various sublayers, we finally obtain a profile of the various ingredients that can reproduce the experimental yield of Cu and S. After this we insert the values

Table 3
Non-resonant cross sections for the reaction $^{32}S(p,p'\gamma)$.

| E (MeV) | $\sigma$ (mb) | $\delta\sigma$ (mb) | E (MeV) | $\sigma$ (mb) | $\delta\sigma$ (mb) |
|---|---|---|---|---|---|
| 3,02 | 0,03977 | 0,01452 | 3,36 | 0,19192 | 0,01841 |
| 3,04 | 0,02577 | 0,00898 | 3,38 | 1,43950 | 0,13712 |
| 3,06 | 0,23653 | 0,06824 | 3,42 | 1,53450 | 0,13520 |
| 3,08 | 0,25029 | 0,05922 | 3,44 | 1,14060 | 0,10047 |
| 3,10 | 0,01927 | 0,00412 | 3,46 | 2,48350 | 0,21872 |
| 3,14 | 0,01071 | 0,00106 | 3,48 | 3,42650 | 0,30158 |
| 3,16 | 0,09512 | 0,00986 | 3,50 | 1,64140 | 0,14436 |
| 3,18 | 0,02363 | 0,00245 | 3,52 | 1,53000 | 0,13447 |
| 3,20 | 0,78035 | 0,07735 | 3,54 | 2,92660 | 0,25698 |
| 3,24 | 0,72974 | 0,07319 | 3,56 | 2,69160 | 0,23625 |
| 3,26 | 0,14226 | 0,01417 | 3,58 | 3,32270 | 0,29156 |
| 3,28 | 0,13537 | 0,01344 | 3,60 | 1,78970 | 0,15692 |
| 3,30 | 0,03131 | 0,00310 | 3,65 | 2,44650 | 0,21433 |
| 3,32 | 0,15241 | 0,01505 | 3,70 | 1,58110 | 0,13841 |
| 3,34 | 0,05080 | 0,00502 | | | |

of depth and atomic concentration we have found to the programme RUMP [9], which manipulates the RBS data at 1,5 MeV for the sample. Again we change those values so that we come to an agreement between the experiment and the simulation. After just two iterations between the two simulating programs, we finally obtain a satisfactory aggreement between the calculated and the experimental profile for Cu and S of the specific sample (figures 4 and 5). Thus, in the case of sample CU11, which is made of an antlerite layer on top of a Cu substrate, we obtain the results presented in Tables 4 and 5.

Applying the same techniques, we analysed the samples named as PATINNA COR, 901 and 901 COR. The results are shown in Tables 6-8.

From the values of Table 6 we observe for the sample PATINNA COR that a very thin layer of copper oxide has been formed in the surface, giving rise to much greater numbers to the copper and oxygen composition in that region than expected. This also does not allow us to go deep enough with backscattering spectrometry, since the scattered protons from sulfur are very few and

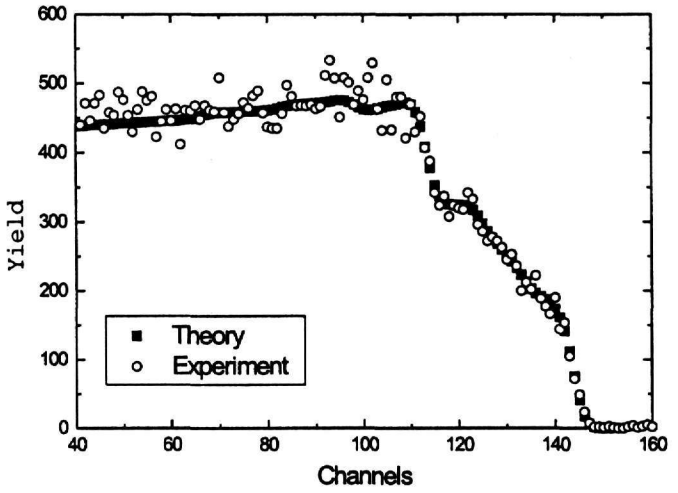


Fig. 4. Backscattering spectrum for the sample CU11.

Table 4
Calculated and experimental yields of S and Cu for the sample CU11.

| E(keV) | Calc. S-Yield (counts/$\mu$Cb) | Exp. S-Yield (counts/$\mu$Cb) | Calc. Cu-Yield (counts/$\mu$Cb) | Exp. Cu-Yield (counts/$\mu$Cb) |
|---|---|---|---|---|
| 3375 | 11,9 | 10,9 $\pm$ 1,1 | 18,5 | 17,2 $\pm$ 1,5 |
| 3380 | 12,1 | 11,3 $\pm$ 1,1 | 19,1 | 18,0 $\pm$ 1,5 |
| 3400 | 66,7 | 66,7 $\pm$ 2,9 | 21,5 | 21,3 $\pm$ 1,4 |
| 3430 | 74,2 | 75,4 $\pm$ 2,8 | 25,3 | 25,3 $\pm$ 1,5 |
| 3460 | 78,3 | 79,3 $\pm$ 3,1 | 29,0 | 28,0 $\pm$ 1,6 |
| 3500 | 74,5 | 73,7 $\pm$ 2,9 | 34,6 | 35,9 $\pm$ 1,9 |
| 3550 | 70,5 | 71,9 $\pm$ 2,7 | 41,9 | 40,1 $\pm$ 1,9 |
| 3600 | 84,6 | 83,5 $\pm$ 3,0 | 48,7 | 47,8 $\pm$ 2,1 |
| 3650 | 79,7 | 80,1 $\pm$ 2,9 | 54,8 | 56,7 $\pm$ 2,4 |
| 3700 | 77,1 | 77,7 $\pm$ 2,8 | 60,4 | 62,4 $\pm$ 2,5 |

the signal they give is covered by the copper background. So we practically see after a certain depth only copper.

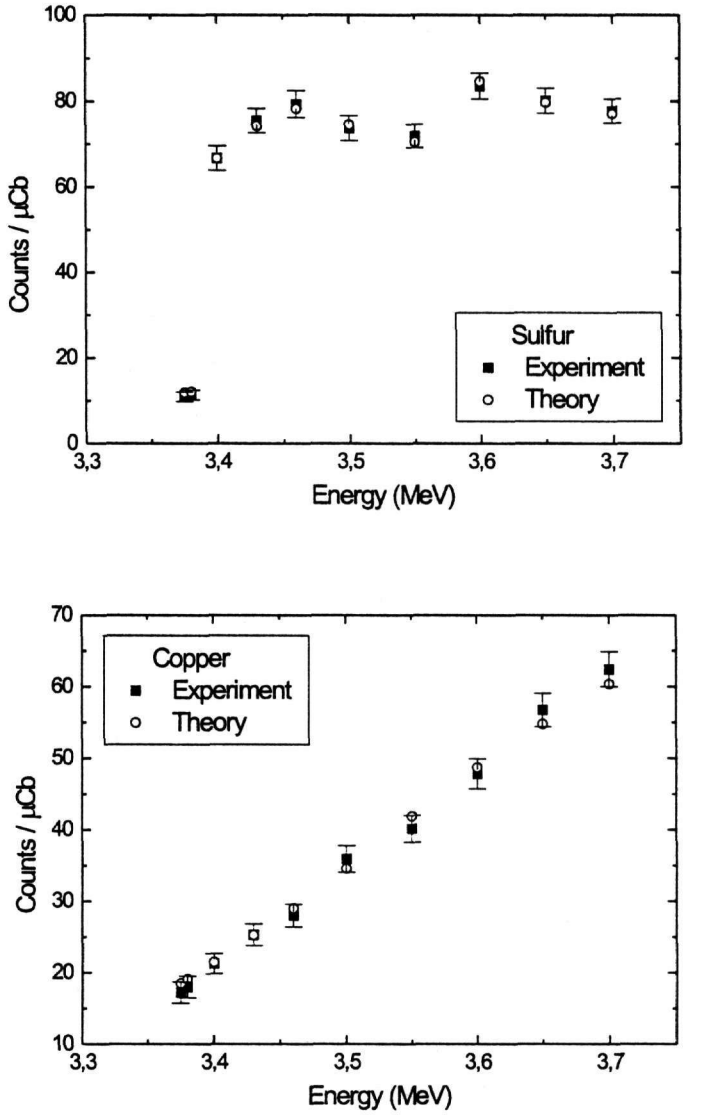


Fig. 5. Experimental yields compared with calculated yields for a) S and b) Cu of sample CU11.

Table 5
Composition of sample CU11.

| Sublayer | Atomic ratio | | | | Thickness ($\mu gr/cm^2$) | Total depth ($\mu gr/cm^2$) |
|---|---|---|---|---|---|---|
| | Cu | S | O | H | | |
| 1 | 2,4 | 1 | 20 | 2 | 140 | 140 |
| 2 | 2,6 | 1 | 17 | 6 | 180 | 320 |
| 3 | 2,8 | 1 | 15 | 6 | 160 | 480 |
| 4 | 3,2 | 1 | 14 | 6 | 150 | 630 |
| 5 | 3,5 | 1 | 12 | 2 | 350 | 980 |
| 6 | 4,5 | 1 | 12 | 2 | 520 | 1500 |
| 7 | 5,0 | 1 | 11 | 6 | 1200 | 2700 |
| 8 | 4,6 | 1 | 8 | 6 | 600 | 3300 |
| 9 | 5,0 | 1 | 10 | 6 | 600 | 3900 |
| 10 | 5,4 | 1 | 12 | 6 | 1600 | 5500 |

Table 6
Composition of sample PATINNA COR.

| Sublayer | Atomic ratio | | | | Thickness ($\mu gr/cm^2$) | Total depth ($\mu gr/cm^2$) |
|---|---|---|---|---|---|---|
| | Cu | S | O | H | | |
| 1 | 1 | 0 | 5 | 0 | 60 | 60 |
| 2 | 9 | 1 | 22 | 8 | 150 | 210 |
| 3 | 9 | 1 | 11 | 4 | 240 | 450 |
| 4 | 11 | 1 | 11 | 4 | 240 | 690 |
| 5 | 11 | 1 | 9 | 4 | 400 | 1090 |
| 6 | 15 | 1 | 2 | 2 | 300 | 1390 |
| 7 | 5 | 1 | 28 | 10 | 1300 | 2690 |
| 8 | 7,5 | 1 | 33 | 10 | 400 | 3090 |
| 9 | 9 | 1 | 40 | 10 | 400 | 3490 |
| 10 | 12 | 1 | 50 | 15 | 400 | 3890 |
| 11 | 15 | 1 | 60 | 15 | 800 | 4690 |
| 12 | 5 | 0 | 1 | 0 | 4000 | 8690 |

Table 7
Composition of sample 901.

| Sublayer | Atomic ratio | | | | Thickness ($\mu gr/cm^2$) | Total depth ($\mu gr/cm^2$) |
|---|---|---|---|---|---|---|
| | Cu | S | O | H | | |
| 1 | 1 | 0 | 4 | 0 | 70 | 70 |
| 2 | 5 | 1 | 14 | 2 | 120 | 190 |
| 3 | 6 | 1 | 11 | 4 | 80 | 270 |
| 4 | 9 | 1 | 10 | 4 | 140 | 410 |
| 5 | 9 | 1 | 5 | 4 | 100 | 510 |
| 6 | 25 | 1 | 13 | 2 | 300 | 810 |
| 7 | 3 | 0 | 1 | 0 | 280 | 1090 |
| 8 | 1 | 0 | 0 | 0 | 650 | 1740 |
| 9 | 15 | 0 | 1 | 0 | 1350 | 3090 |
| 10 | 5 | 0 | 1 | 0 | 10000 | 13090 |

Table 8
Composition of sample 901 COR.

| Sublayer | Atomic ratio | | Thickness ($\mu gr/cm^2$) | Total depth ($\mu gr/cm^2$) |
|---|---|---|---|---|
| | Cu | O | | |
| 1 | 1,7 | 1 | 300 | 300 |
| 2 | 2,5 | 1 | 270 | 570 |
| 3 | 3,7 | 1 | 510 | 1080 |
| 4 | 3,3 | 1 | 500 | 1580 |
| 5 | 4 | 1 | 370 | 1950 |
| 6 | 4,8 | 1 | 770 | 2720 |
| 7 | 5 | 1 | 850 | 3570 |
| 8 | 4,2 | 1 | 640 | 4210 |
| 9 | 2 | 1 | 2000 | 6210 |
| 10 | 1 | 0 | 20000 | 26210 |

## 7 Conclusions

This work has demonstrated that the combined use of RBS and NRA can lead to a consistent description of inhomogeneous layer structures. This combination takes advantage of the different depth resolution of the two techniques. Samples of widely differing composition can be analysed. It was also demonstrated that finer steps in the NRA measurements are necessary for better resolution. A final point which became apparent is that cross sections of interesting nuclear reactions have to be measured again in more detail with the applications in mind. Most of the data currently available in the literature were obtained for purposes of nuclear spectroscopy. Hence they are either relative or fragmentary.

## Acknowledgements

Thanks should be expressed to Prof. P. Missailides for making the samples available, as well as to the Tandem Accelerator crew for their assistance during the long-range measurements.

## References

[1] V.H. Rotberg, Nucl. Instr. and Meth. 200 (1982) 511.

[2] J. Raisanen and R. Lapatto, Nucl. Instr. and Meth. B 30 (1988) 90.

[3] C. Tsartsarakos, P. Misaelides and A. Katsanos, Nucl. Instr. and Meth. B 45 (1990) 33.

[4] J.W. Olness et al., Phys. Rev. 112 (1958) 1702.

[5] M.E. Sevior et al., Aust. J. Phys. 36 (1983) 463.

[6] C.E. Rolfs and W.S. Rodney, Cauldrons in the Cosmos (The University of Chicago Press, 1988).

[7] R.L. Auble, Nucl. Data Sheets 28 (1979) 559.

[8] G. Kaliambakos, PGAMMA code (1999), unpublished.

[9] L.R. Doolittle, Nucl. Instr. and Meth. B 9 (1985) 344.